

Three-dimensional, one-point collision with friction

Shlomo Djerassi

Received: 10 February 2011 / Accepted: 17 November 2011 / Published online: 31 December 2011
© Springer Science+Business Media B.V. 2011

Abstract This paper deals with one-point collision with friction in three-dimensional, simple non-holonomic multibody systems. With Keller's idea regarding the normal impulse as an independent variable during collision, and with Coulomb's friction law, the system equations of motion reduce to five, coupled, nonlinear, first order differential equations. These equations have a singular point if sticking is reached, and their solution is 'navigated' through this singularity in a way leading to either sticking or sliding renewal in a uniquely defined direction. Here, two solutions are presented in connection with Newton's, Poisson's and Stronge's classical collision hypotheses. One is based on numerical integration of the five equations. The other, significantly faster, replaces the integration by a recursive summation. In connection with a two-sled collision problem, close agreement between the two solutions is obtained with a few summation steps.

Keywords Collision with friction · Coulomb's friction hypothesis · Newton's collision hypothesis · Poisson's collision hypothesis · Stronge's collision hypothesis · Hodograph

1 Introduction

This paper deals with one-point, 'hard' collision with friction in three-dimensional (3D), simple non-holonomic multibody systems, using classical collision theories (alternate approaches involving restoring and dissipative forces, also called 'soft' approach, and finite-element-based approach, also called full-deformation approach, described, e.g., by Chatterjee and Ruina in [1] and by Najafabadi et al. in [2], will not be discussed here). Djerassi has shown in [3] that, as far as two-dimensional (2D) systems are concerned, an algebraic, closed form, Poisson's and Stronge's hypotheses-related solutions always exist, and are unique, coherent, and energy-consistent.

Unfortunately, this is not the case with collision in 3D systems. If Keller's idea [4] and Coulomb's friction law are applied to the solution of collision problems, one obtains a set

S. Djerassi (✉)
Rafael, P.O.Box 2250 Haifa, Israel
e-mail: shlomod@rafael.co.il

of five, coupled, nonlinear, first order differential equations, which has a singular point if sticking is reached. Solutions with analytic integrals exist only in special cases (e.g., in the absence of friction, as in [5] and [6], or if the ‘reduced’ 3×3 mass matrix is diagonal [7]). Battle shows in [8] that for what he calls ‘balanced collision’, solutions can be obtained with the integration of a single differential equation, that the remaining unknowns can be evaluated algebraically; and that sliding renewal cannot occur. He shows that, for a given system and collision points, the hodographs (describing the sliding relative velocity components of the colliding points versus one another) spanned by the collision initial conditions are continuous, unique and nonintersecting curves.

Thus, 3D collision problems require in general the solution of the five differential equations, investigated in depth by a small number of authors. Bhatt and Koechling [9] used Keller’s idea ([4]) to formulate the differential equations governing 3D collision of a rigid body hitting a plane, pointing out the singularity encountered if sticking occurs; and, showed that, depending on the coefficient of friction, either sticking prevails, or sliding is resumed in a constant, predictable direction. Battle [10] exploits the mathematical similarity between the description of the hodograph and an autonomous nonlinear flow, and, without solving the associated differential equations, draws a picture of the hodograph behavior during the sliding phase of the collision, and its dependence on five system parameters and on the coefficient of friction. Stronge [11] formulated the differential equations governing collisions between two bodies, and, introducing his coefficient of restitution, solved a number of examples (e.g., ball, rod, triangle and spherical pendulum hitting a plane). Zhen and Liu [12] formulated differential equations for 3D collision of holonomic systems using Keller’s idea, replacing the numerical integration with a difference method. They used a search algorithm to find the sliding direction if sliding resumption occurs.

It may be concluded that these authors provided the building blocks required to produce comprehensive solutions to the 3D, one point collision with friction problem for simple non-holonomic systems, a task undertaken in the present work. Two complete solutions are discussed, the first is based on the numerical integration of the indicated five differential equations, dealing with sliding, sticking and sliding renewal phases; and the second comprises a recursive summation associated with the first.

In both solutions, use is made of the classic collision hypotheses (by Newton [13], Poisson [14] and Stronge/Boulanger [11, 15], introducing, respectively, ‘kinematic’, ‘kinetic’ and ‘energetic’ coefficients of restitutions), a choice requiring elaborations in view of two observations related to these hypotheses. First, these hypotheses capture local effects, i.e., elastic and plastic deformations in the neighborhood of the colliding points. When applied to one point collision problems in multibody systems, they ‘disregard’ the effect of the collision on the entire system (namely, on the rise of structural vibrations, friction in joints, restitution in the tangential direction, etc., as noted, e.g., in [16] and [1]), hence are not accurate. Second, Newton’s collision hypothesis can lead to an increase of the system mechanical energy (illustrated by Kane and Levinson in [17]). These observations gave rise to a number of newly defined hypotheses. For example, Chatterjee and Ruina augment in [1] Newton’s hypothesis with a tangential coefficient of restitution, which, among other features, improves the predictions of certain experimental results. Najafabadi et al. propose in [16] a new energy-related coefficient of restitution, which equals the square root of the ratio of the kinetic energy associated with the ‘constrained’ motion before and after the collision, better accommodating multibody systems. Rubin [18] discusses physical restrictions on the coefficient of restitution, concluding that it equals the ratio between the components of the velocity of separation and the velocity of approach in the impulse direction. Ivanov [19] arrives at a similar definition from an energy-related view-point.

In spite of their shortcomings, the classical hypotheses are widely used by numerous authors to conduct their studies. For example, Whittaker [5], Brach [20] and Smith [7] use Newton’s hypothesis, Routh [21], Keller [4] and Zen and Liu [12] use Poisson’s hypothesis, and Stronge [11], Hurmuzlu [22] and Djerassi [3] use Stronge/Boulanger’s hypothesis. Marghitu and Hurmuzlu [23], Smith and Liu [24], Ivanov [19] and others discuss all three hypotheses, showing that they lead to different results. It is understood, therefore, that a real-world problem requires calibration of the coefficient of restitution, validating its value for a limited parameter range (including, as shown by Stoianovici and Hurmuzlu in [25], geometrical ones). Incidentally, parameters associated with ‘soft’ approaches also require calibration (as e.g., in [26] and [27]). Accordingly, the analysis described here rests on the classical hypotheses. The paper starts with preliminaries (Sect. 2), followed by a presentation of the five differential equations and their solution in the events of sliding, sticking and sliding renewal (Sect. 3) in conjunction with the three classical hypotheses (Sect. 4). A 3D two-sled collision example is solved by integration in Sect. 5, and then by a recursive summation in Sect. 6. A short discussion in Sect. 7 concludes this work.

2 Preliminaries

Let

$$F_r + F_r^* = 0 \quad (r = 1, \dots, p) \tag{1}$$

be Kane’s equations of motion for S , a simple, non-holonomic system of ν particles $P_i (i = 1, \dots, \nu)$ of mass m_i , possessing p independent generalized speeds u_1, \dots, u_p and $n (n > p)$ generalized coordinates q_1, \dots, q_n , where F_r and F_r^* are, respectively, the r th generalized active force and the r th generalized inertia force for S (Kane and Levinson [17]). \mathbf{v}^{P_i} , the velocity of P_i in N , a Newtonian reference frame, can be expressed in terms of $u_1, \dots, u_p, q_1, \dots, q_n$ and time t as

$$\mathbf{v}^{P_i} = \sum_{r=1}^p \mathbf{v}_r^{P_i} u_r + \mathbf{v}_t^{P_i} \quad (i = 1, \dots, \nu) \tag{2}$$

where $\mathbf{v}_r^{P_i}$, called the r th partial velocity of P_i , and $\mathbf{v}_t^{P_i}$, called the remainder partial velocity of P_i , are vector functions of q_1, \dots, q_n and t . Let B and B' be bodies of S , and let P be a point of B coming into contact with point P' of B' during the collision of B with B' occurring between two instants t_1 and t_2 (Fig. 1). Under these circumstances, collision

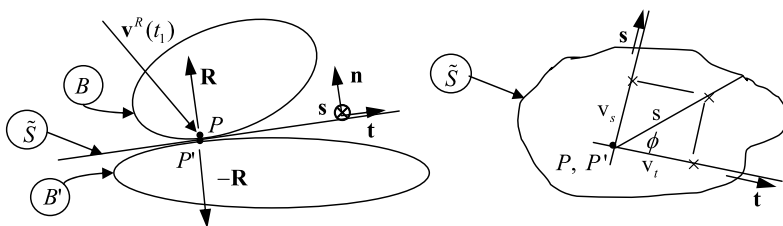


Fig. 1 3D Collision; side (left) and top views on \tilde{S}

hypotheses [11, 13, 14] can be used to bring the effect of this collision into (1). To this end, let \mathbf{v}^R be the relative velocity of points P and P' , defined as

$$\mathbf{v}^R \triangleq \mathbf{v}^P - \mathbf{v}^{P'}, \tag{3}$$

and note that \mathbf{v}^R can be written similarly to \mathbf{v}^{P_i} in (2), hence

$$\mathbf{v}_r^R = \mathbf{v}_r^P - \mathbf{v}_r^{P'} \quad (r = 1, \dots, p), \tag{4a}$$

$$\mathbf{v}_t^R = \mathbf{v}_t^P - \mathbf{v}_t^{P'}, \tag{4b}$$

where \mathbf{v}_r^R is the coefficient of u_r in \mathbf{v}^R . Suppose that, during collision, P' exerts on P a force \mathbf{R} , so that P exerts on P' a force $-\mathbf{R}$. Then (1) give way to equations that bring into evidence the contributions of \mathbf{R} , i.e.,

$$F_r + F_r^* + \mathbf{R} \cdot \mathbf{v}_r^P - \mathbf{R} \cdot \mathbf{v}_r^{P'} = 0 \quad (r = 1, \dots, p; t_1 \leq t \leq t_2) \tag{5}$$

or, in view of (4a),

$$F_r + F_r^* + \mathbf{R} \cdot \mathbf{v}_r^R = 0 \quad (r = 1, \dots, p). \tag{6}$$

During the collision, P is assumed to maintain contact with P' , i.e., to coincide with P' ; and a plane \tilde{S} exists which passes through $P' (\equiv P)$ and is tangent to B and B' at P' if both are locally smooth, or to B' at P' if only B' is locally smooth. Name B and B' such that \mathbf{n} , a unit vector perpendicular to \tilde{S} , makes $\mathbf{v}^R(t_1) \cdot \mathbf{n}$ a non-positive quantity.

Align \mathbf{t} , a unit vector lying in \tilde{S} , with the projection of $\mathbf{v}^R(t_1)$ on \tilde{S} , making $\mathbf{v}^R(t_1) \cdot \mathbf{t}$ a non-negative quantity (see Fig. 1) and $\mathbf{v}^R(t_1) \cdot \mathbf{s}$, where $\mathbf{s} \triangleq \mathbf{n} \times \mathbf{t}$, vanish. Then

$$\mathbf{v}^R(t) = \mathbf{v}^R(t) \cdot \mathbf{nn} + \mathbf{v}^R(t) \cdot \mathbf{tt} + \mathbf{v}^R(t) \cdot \mathbf{ss}, \tag{7a}$$

$$\mathbf{v}^R(t_1) \cdot \mathbf{n} \leq 0, \tag{7b}$$

$$\mathbf{v}^R(t_1) \cdot \mathbf{t} \geq 0, \tag{7c}$$

$$\mathbf{v}^R(t_1) \cdot \mathbf{s} = 0. \tag{7d}$$

$\mathbf{v}^R(t_1)$ and $\mathbf{v}^R(t_2)$ (at times denoted \mathbf{v}^A and \mathbf{v}^S [17]) are called velocity of approach and velocity of separation, respectively. Equation (6) can thus be replaced with

$$F_r + F_r^* + \mathbf{R} \cdot \mathbf{nv}_r^R \cdot \mathbf{n} + \mathbf{R} \cdot \mathbf{tv}_r^R \cdot \mathbf{t} + \mathbf{R} \cdot \mathbf{sv}_r^R \cdot \mathbf{s} = 0 \quad (r = 1, \dots, p; t_1 \leq t \leq t_2). \tag{8}$$

If it is assumed that $t_2 - t_1$ is ‘small’ compared to time constants associated with the motion of S , and that, consequently, q_1, \dots, q_n and t remain constants between t_1 and t_2 , then both sides of (8) can be integrated from t_1 to $t \leq t_2$, yielding

$$\sum_{s=1}^p m_{rs} \Delta u_s + I_n \mathbf{v}_r^R \cdot \mathbf{n} + I_t \mathbf{v}_r^R \cdot \mathbf{t} + I_s \mathbf{v}_r^R \cdot \mathbf{s} = 0 \quad (r = 1, \dots, p). \tag{9}$$

Here, I_n , I_t and I_s are the normal and tangential impulses at time t , defined as

$$I_n \triangleq \left(\int_{t_1}^t \mathbf{R} dt \right) \cdot \mathbf{n}, \tag{10a}$$

$$I_t \hat{=} \left(\int_{t_1}^{t'} \mathbf{R} dt \right) \cdot \mathbf{t}, \tag{10b}$$

$$I_s \hat{=} \left(\int_{t_1}^{t'} \mathbf{R} dt \right) \cdot \mathbf{s}, \tag{10c}$$

$\mathbf{v}_r^R \hat{=} \mathbf{v}_r^R(t)$ ($t_1 \leq t \leq t_2, r = 1, \dots, p$) (see (4a)), Δu_s ($s = 1, \dots, p$) are defined as

$$\Delta u_s \hat{=} u_s(t) - u_s(t_1) \quad (s = 1, \dots, p), \tag{11}$$

and m_{rs} is the entry in row r , column s of the mass matrix $-\mathbf{M}$ associated with (1) (see (63), Appendix A). Note that \mathbf{n}, \mathbf{t} and \mathbf{s} , defined only for $t_1 \leq t \leq t_2$, remain fixed in N during the collision. Also note that $\mathbf{R} \cdot \mathbf{n}(t_1 \leq t \leq t_2) > 0$ (P' cannot ‘pull’ P), hence $I_n > 0$. The matrix form of (9), solved for Δu_s ($s = 1, \dots, p$) reads

$$|\Delta u_1 \cdots \Delta u_p| = -\mathbf{V}_n \mathbf{M}^{-1} I_n - \mathbf{V}_n \mathbf{M}^{-1} I_t - \mathbf{V}_n \mathbf{M}^{-1} I_s \tag{12a}$$

$$\mathbf{V}_n \hat{=} |\mathbf{v}_1^R \cdot \mathbf{n} \cdots \mathbf{v}_p^R \cdot \mathbf{n}|, \tag{12b}$$

$$\mathbf{V}_t \hat{=} |\mathbf{v}_1^R \cdot \mathbf{t} \cdots \mathbf{v}_p^R \cdot \mathbf{t}|, \tag{12c}$$

$$\mathbf{V}_s \hat{=} |\mathbf{v}_1^R \cdot \mathbf{s} \cdots \mathbf{v}_p^R \cdot \mathbf{s}|. \tag{12d}$$

Now, $\mathbf{v}^R(t) - \mathbf{v}^R(t_1)$ can be written

$$\mathbf{v}^R(t) - \mathbf{v}^R(t_1) = |\Delta u_1 \cdots \Delta u_p| |\mathbf{v}_1^R \cdots \mathbf{v}_p^R|^T \quad (\mathbf{v}_t^R(t) - \mathbf{v}_t^R(t_1) \stackrel{(4b)}{=} 0) \tag{13}$$

when use is made of (2), (4a) and (4b). If both sides of (13) are dot-multiplied by \mathbf{n}, \mathbf{t} and \mathbf{s} , one at a time, and if $|\Delta u_1 \cdots \Delta u_p|$ is eliminated with the aid of (12a), one has, defining $\mathbf{V} \hat{=} |\mathbf{V}_n \mathbf{V}_t \mathbf{V}_s|^T$ ($\Rightarrow \mathbf{V}^T = |\mathbf{V}_n^T \mathbf{V}_t^T \mathbf{V}_s^T|$),

$$\begin{vmatrix} \mathbf{v}^R(t) \cdot \mathbf{n} - \mathbf{v}^R(t_1) \cdot \mathbf{n} \\ \mathbf{v}^R(t) \cdot \mathbf{t} - \mathbf{v}^R(t_1) \cdot \mathbf{t} \\ \mathbf{v}^R(t) \cdot \mathbf{s} - \mathbf{v}^R(t_1) \cdot \mathbf{s} \end{vmatrix} = -\mathbf{V} \mathbf{M}^{-1} \mathbf{V}^T \begin{vmatrix} I_n \\ I_t \\ I_s \end{vmatrix}. \tag{14}$$

The coefficients of I_n, I_t and I_s in (14) are functions of q_1, \dots, q_n and t , hence remain constants between t_1 and t_2 . Defining $m_{nn}, m_{nt}, m_{tt}, m_{ns}, m_{ts}$ and m_{ss} as

$$\begin{aligned} m_{nn} \hat{=} -\mathbf{V}_n \mathbf{M}^{-1} \mathbf{V}_n^T > 0, \quad m_{nt} \hat{=} -\mathbf{V}_n \mathbf{M}^{-1} \mathbf{V}_t^T, \quad m_{tt} \hat{=} -\mathbf{V}_t \mathbf{M}^{-1} \mathbf{V}_t^T > 0, \\ m_{ns} \hat{=} -\mathbf{V}_n \mathbf{M}^{-1} \mathbf{V}_s^T, \quad m_{ts} \hat{=} -\mathbf{V}_t \mathbf{M}^{-1} \mathbf{V}_s^T, \quad m_{ss} \hat{=} -\mathbf{V}_s \mathbf{M}^{-1} \mathbf{V}_s^T > 0, \end{aligned} \tag{15}$$

$v_n, v_t, v_s, v_{n1}, v_{t1}, v_{s1}, v_{n2}, v_{t2}$ and v_{s2} , the \mathbf{n}, \mathbf{t} and \mathbf{s} components of \mathbf{v}^R at times t, t_1 and t_2 , and I_{n2}, I_{t2} and I_{s2} , the \mathbf{n}, \mathbf{t} and \mathbf{s} impulse components at time t_2 , as

$$v_n \stackrel{(7a)}{\hat{=}} \mathbf{v}^R(t) \cdot \mathbf{n}, \quad v_t \stackrel{(7a)}{\hat{=}} \mathbf{v}^R(t) \cdot \mathbf{t}, \quad v_s \stackrel{(7a)}{\hat{=}} \mathbf{v}^R(t) \cdot \mathbf{s}, \tag{16}$$

$$v_{n1} \stackrel{(7b)}{\hat{=}} \mathbf{v}^R(t_1) \cdot \mathbf{n} (< 0), \quad v_{t1} \stackrel{(7c)}{\hat{=}} \mathbf{v}^R(t_1) \cdot \mathbf{t} (> 0), \quad v_{s1} \stackrel{(7d)}{\hat{=}} \mathbf{v}^R(t_1) \cdot \mathbf{s} (= 0), \tag{17}$$

$$v_{n2} \hat{=} \mathbf{v}^R(t_2) \cdot \mathbf{n}, \quad v_{t2} \hat{=} \mathbf{v}^R(t_2) \cdot \mathbf{t}, \quad v_{s2} \hat{=} \mathbf{v}^R(t_2) \cdot \mathbf{s}, \tag{18}$$

$$I_{n2} \hat{=} I_n(t_2), \quad I_{t2} \hat{=} I_t(t_2), \quad I_{s2} \hat{=} I_s(t_2), \tag{19}$$

($I_{n1} \hat{=} I_n(t_1) = 0, I_{t1} \hat{=} I_t(t_1) = 0, I_{s1} \hat{=} I_s(t_1) = 0$) one can rewrite (14) for $t_1 \leq t \leq t_2$

$$v_n - v_{n1} = m_{nn}I_n + m_{nt}I_t + m_{ns}I_s, \tag{20}$$

$$v_t - v_{t1} = m_{nt}I_n + m_{tt}I_t + m_{ts}I_s, \tag{21}$$

$$v_s - v_{s1} = m_{ns}I_n + m_{ts}I_t + m_{ss}I_s. \tag{22}$$

(Equations (20)–(22) reduce to (22)–(23) in [28] for 2D systems; then $m_{ts} = m_{ns} = m_{ss} = 0$.) These so-called ‘reduced equations of motion’ possess a coefficient matrix \mathfrak{M} shown in Appendix A to be positive definite; and six unknowns I_n, I_t, I_s, v_n, v_t and v_s . Knowledge of I_{n2}, I_{t2} and I_{s2} enables the evaluation of $\Delta u_1(t_2) \dots \Delta u_p(t_2)$ with (12a), with which simulations (i.e., numerical integrations of (1)) can be kept running. Accordingly, I_{n2}, I_{t2} and I_{s2} are generated in the following sections first by integration and then by recursive summation, with the aid of friction- and collision-related hypotheses.

Regarding ΔE_2 , the change in the system mechanical energy following a collision, a straightforward extension of the proof given in [28] for the planar case shows that

$$\Delta E_2 = 1/2I_{n2}(v_{n2} + v_{n1}) + 1/2I_{t2}(v_{t2} + v_{t1}) + 1/2I_{s2}(v_{s2} + v_{s1}) \tag{23}$$

($= 1/2\mathbf{u}_2(-\mathbf{M})\mathbf{u}_2^T - 1/2\mathbf{u}_1(-\mathbf{M})\mathbf{u}_1^T$, where $\mathbf{u} \hat{=} |u_1 \dots u_p|$) for the 3D case, provided

$$-I_{n2}\mathbf{v}_t^R \cdot \mathbf{n} - I_{t2}\mathbf{v}_t^R \cdot \mathbf{t} - I_{s2}\mathbf{v}_t^R \cdot \mathbf{s} + \sum_{i=1}^{\nu} m_i \mathbf{v}_t^{P_i} \cdot [\mathbf{v}^{P_i}(t_2) - \mathbf{v}^{P_i}(t_1)] \stackrel{(2)}{=} 0, \tag{24}$$

a condition ‘neutralizing’ specified motions implied by \mathbf{v}_t^R and $\mathbf{v}_t^{P_i}$ ($i = 1, \dots, \nu$).

3 Solution by integration

One can start with the differential form of (20)–(22) given by

$$dv_n = m_{nn}dI_n + m_{nt}dI_t + m_{ns}dI_s, \tag{25}$$

$$dv_t = m_{nt}dI_n + m_{tt}dI_t + m_{ts}dI_s, \tag{26}$$

$$dv_s = m_{ns}dI_n + m_{ts}dI_t + m_{ss}dI_s. \tag{27}$$

Let the slip speed s of P relative to P' and the orientation angle ϕ be defined so that

$$v_t = sc\phi, \tag{28a}$$

$$dv_t = c\phi ds - s\phi d\phi, \tag{28b}$$

$$v_s = ss\phi, \tag{28c}$$

$$dv_s = s\phi ds + sc\phi d\phi, \tag{28d}$$

where $s\phi = \sin \phi$ and $c\phi = \cos \phi$ (Fig. 1); and note that as long as there is slip $\mathbf{R} \cdot \mathbf{t} = -\mu \mathbf{R} \cdot \mathbf{nc}\phi$, $\mathbf{R} \cdot \mathbf{s} = -\mu \mathbf{R} \cdot \mathbf{ns}\phi$ ($[(\mathbf{R} \cdot \mathbf{t})^2 + (\mathbf{R} \cdot \mathbf{s})^2]^{1/2} = \mu |\mathbf{R} \cdot \mathbf{n}|$), in accordance with Coulomb's friction law, or, in view of (10a)–(10c),

$$dI_t = -\mu dI_n c\phi, \quad dI_s = -\mu dI_n s\phi, \tag{29}$$

where μ is Coulomb's coefficient of friction. With f, g and h defined as

$$\begin{aligned} f &\hat{=} dv_n/dI_n, & g &\hat{=} dv_t/dI_n c\phi + dv_s/dI_n s\phi, \\ h &\hat{=} -dv_t/dI_n s\phi + dv_s/dI_n c\phi \end{aligned} \tag{30}$$

one can show, dividing (25)–(27) throughout by dI_n and using (29), that

$$f = m_{nn} - \mu m_{nt} c\phi - \mu m_{ns} s\phi, \tag{31}$$

$$g = m_{nt} c\phi + m_{ns} s\phi - \mu m_{tt} c^2\phi - \mu m_{ss} s^2\phi - 2\mu m_{ts} s\phi c\phi, \tag{32}$$

$$h = -m_{nt} s\phi + m_{ns} c\phi - \mu m_{ts} (c^2\phi - s^2\phi) + \mu (m_{tt} - m_{ss}) s\phi c\phi, \tag{33}$$

and that dv_t and dv_s can be eliminated from (25), (28b) and (28d), which reduce to

$$d\phi/dI_n = h/s, \tag{34a}$$

$$ds/dI_n = g, \tag{34b}$$

$$dv_n/dI_n = f, \tag{34c}$$

$$dI_t/dI_n = -\mu c\phi, \tag{34d}$$

$$dI_s/dI_n = -\mu s\phi. \tag{34e}$$

Equations (34a)–(34e) comprise five ordinary, coupled, first order differential equations with five dependent variables ϕ, s, v_n, I_t and I_s and one, monotonously increasing, independent variable I_n governing the sliding portion of the collision. The right-hand sides of (34a)–(34e) and their partial derivatives with respect to ϕ, s, v_n, I_t and I_s , are continuous functions of ϕ, s, v_n, I_t and I_s in the region $s > 0$. Therefore, a solution of (34a)–(34e) in conjunction with the following initial conditions (when $I_n = 0$): $\phi(0) = 0, s(0) = v_{t1}$ (then, by (28a)–(28d) $v_t(0) = s(0) = v_{t1}, v_s(0) = 0, v_n(0) = v_{n1}, I_t(0) = 0$ and $I_s(0) = 0$, always exists and is unique (see, e.g., [29], p. 267). Moreover, $d\Delta E = \mathbf{R} \cdot \mathbf{v}^R(t) = (\mathbf{R} \cdot \mathbf{nn} + \mathbf{R} \cdot \mathbf{tt} + \mathbf{R} \cdot \mathbf{ss}) \cdot (v_n \mathbf{n} + v_t \mathbf{t} + v_s \mathbf{s}) \stackrel{(7a),(16)}{=} (v_n - \mu s) dI_n$. With $d\Delta E_n \hat{=} v_n dI_n$, (34a)–(34e) can be augmented with the differential equations

$$d\Delta E/dI_n = v_n - \mu s, \tag{35a}$$

$$d\Delta E_n/dI_n = v_n, \tag{35b}$$

enabling the evaluation of the ‘total’ and the ‘normal’ energy losses during collision.

It is worth noting that (23) is valid for $t_1 < t \leq t_2$ if $\Delta E_2, I_{n2}, v_{t2}$, etc. are replaced with $\Delta E, I_n, v_t$, etc.; then the I_n derivative of both sides of (23) can be used to prove the validity of (35a) with the aid of (29), (34b)–(34e) and (20)–(22) in yet a different way. Moreover, $d[1/2I_n(v_n + v_{n1})]/dI_n \neq v_n$, hence $\Delta E_n \neq 1/2I_n(v_n + v_{n1})$. It can be shown this is also the case with 2D systems, except in sliding.

In general (34a)–(34e) cannot be integrated analytically (see, e.g., [9] and [11]). Furthermore, the ‘trivial’ solution $\phi \equiv 0$, valid for 2D problems, does not apply: $\phi \equiv 0$ implies $d\phi/dI_n = 0$; however, during sliding $s > 0$, hence $h(\mu, \phi) = 0$ (see (34a)). This equation has at least two nonzero solutions for ϕ (Appendix B), in contrast with the trivial solution.

Collisions comprise at least the first of the following events.

3.1 Sliding

Suppose that I_{n2} , the normal impulse at t_2 is known, and that the sliding speed s remains positive throughout the integration of (34a)–(34e) from $I_n = 0$ to $I_n = I_{n2}$. Then integration underlies the solution for sliding, yielding $\phi(t_2)$, $s(t_2) (> 0)$ (hence, by (28a) and (28c) v_{t2} and v_{s2}), v_{n2} , I_{t2} and I_{s2} .

3.2 Sticking

It may occur that s becomes zero, say, at $t = t_s < t_2$, i.e., before $I_n = I_{n2}$. In that event $h(\mu, \phi) \rightarrow 0$ as $s \rightarrow 0$, provided $g(\mu, \phi) < 0$; and vice versa. To show this, note that

$$dv_t/dI_n \stackrel{(28b)}{=} c\phi ds/dI_n - s\phi d\phi/dI_n \stackrel{(34a,b)}{=} gc\phi - hs\phi, \tag{36a}$$

$$dv_s/dI_n \stackrel{(28d)}{=} s\phi ds/dI_n + s\phi d\phi/dI_n \stackrel{(34a,b)}{=} gs\phi + hc\phi, \tag{36b}$$

hence

$$dv_s/dv_t = (dv_s/dI_n)/(dv_t/dI_n) = (gs\phi + hc\phi)/(gc\phi - hs\phi). \tag{37}$$

Moreover, $\lim_{s \rightarrow 0} (dv_s/dv_t) \stackrel{(28b,d)}{=} \lim_{s \rightarrow 0} [s(\phi)/c(\phi)]$, so that, with (37),

$$\begin{aligned} &\lim_{s \rightarrow 0} [s\phi/c\phi - (gs\phi + hc\phi)/(gc\phi - hs\phi)] \\ &= \lim_{s \rightarrow 0} \{h/[c\phi(gc\phi - hs\phi)]\} = 0 \quad \Rightarrow \quad h(\mu, \phi)|_{s=0} = 0 \end{aligned}$$

provided at least one solution $\bar{\phi}$ of $h(\mu, \phi) = 0$ satisfies $g(\mu, \bar{\phi})c^2\bar{\phi} \neq 0$. In fact, when $s (> 0) \rightarrow 0$ then necessarily $ds/dI_n < 0$, hence, by (34b), $\lim_{s \rightarrow 0 \Rightarrow \phi \rightarrow \bar{\phi}} g(\mu, \phi) < 0$, in agreement with Appendix B, showing that at least one such solution exists. Conversely, (34a) and (34b) can be condensed into

$$ds/s = g/hd\phi, \tag{38}$$

an equation which, when integrated from $s = s(0)$ and $\phi = 0$ to s and ϕ yields $s = s(0) \exp \int_0^\phi g(\mu, \eta)/h(\mu, \eta) d\eta$, showing that if $\lim_{\phi \rightarrow \bar{\phi}} h(\mu, \phi) \rightarrow 0$ (and, since $d\eta/h \stackrel{(34a)}{>} 0$) and $\lim_{\phi \rightarrow \bar{\phi}} g(\mu, \phi) < 0$, then $s (> 0) \rightarrow 0$ and sticking is approached.

During sticking, (25)–(27) remain valid with

$$v_t \equiv 0, \quad v_s \equiv 0 \quad \Rightarrow \quad dv_t = 0, \quad dv_s = 0, \tag{39}$$

yielding, when solved for dI_n , dI_t and dI_s ,

$$dI_n = c_n dv_n, \tag{40a}$$

$$dI_t = c_t dv_n, \tag{40b}$$

$$dI_s = c_s dv_n, \tag{40c}$$

where c_n, c_t and c_s are functions of $m_{nn}, m_{nt}, \dots, m_{ss}$ given by

$$c_n = (m_{tt}m_{ss} - m_{ts}^2) / \det \mathfrak{M} > 0, \tag{41a}$$

$$c_t = (m_{ns}m_{ts} - m_{nt}m_{ss}) / \det \mathfrak{M}, \tag{41b}$$

$$c_s = (m_{nt}m_{ts} - m_{ns}m_{tt}) / \det \mathfrak{M}, \tag{41c}$$

$$\Rightarrow \mathfrak{M} |c_n c_t c_s|^T = |100|^T. \tag{41d}$$

Equations (40a)–(40c) govern sticking just as (34c)–(34e) govern sliding. Seeking limit-values of ϕ and μ satisfying both (34c, 34d, 34e) and (40a)–(40c) one finds

$$dI_s/dI_t \stackrel{(34d,e)}{=} \tan \phi \stackrel{(40)}{=} c_s/c_t, \tag{42}$$

$$\mu \stackrel{(34d)}{=} -dI_t/dI_n c^{-1} \phi \stackrel{(40a,b)}{=} -c_t/(c_n c \phi), \quad \mu \stackrel{(34e)}{=} -dI_s/dI_n s^{-1} \phi \stackrel{(40a,c)}{=} -c_s/(c_n s \phi).$$

Here $c_n > 0$ (see (41a)) and $\mu > 0$, conditions that, given c_t and c_s , determine μ and (the signs of $s\phi$ and $c\phi$, hence) ϕ uniquely, namely,

$$\mu_c = \sqrt{c_t^2 + c_s^2/c_n}, \quad \phi_c = a \tan 2(-c_s, -c_t). \tag{43}$$

Moreover, $dv_t/dI_n = 0$ and $dv_s/dI_n = 0$ ((39)), so that, in view of (36a) and (36b)

$$g(\mu, \phi) = 0, \quad h(\mu, \phi) = 0. \tag{44}$$

μ_c and ϕ_c in (43) satisfy (44), and conversely, if $g(\mu, \phi)$ and $h(\mu, \phi)$ ((32) and (33)) are substituted explicitly in (36a) and (36b), then, in view of (39) and (44), $m_{ns} - \mu m_{ss} s \phi - \mu m_{ts} c \phi = 0$ and $m_{nt} - \mu m_{tt} c \phi - \mu m_{ts} s \phi = 0$, equations having (μ_c, ϕ_c) as a unique solution. μ_c is interpreted as the minimal coefficient of friction for which sticking remains once it has occurred. (In ‘balanced collision’ $m_{nt} = m_{ns} = 0 \stackrel{(41)}{\Rightarrow} c_t = c_s = 0 \stackrel{(43)}{\Rightarrow} \mu_c = 0$, as indicated by Battle in [8].) That is, if $s(t = t_S) = 0$ and $\mu > \mu_c$ then $s(t_S < t \leq t_2) = 0$; and, for $t_S < t \leq t_2$, (34a)–(34e) can be replaced with

$$d\phi/dI_n = 0, \tag{45a}$$

$$ds/dI_n = 0, \tag{45b}$$

$$dv_n/dI_n \stackrel{(40a)}{=} 1/c_n, \tag{45c}$$

$$dI_t/dI_n \stackrel{(40a,b)}{=} c_t/c_n, \tag{45d}$$

$$dI_s/dI_n \stackrel{(40a,c)}{=} c_s/c_n. \tag{45e}$$

3.3 Sliding renewal

If $\mu < \mu_c$, and $s(t = t_S) = 0$ before I_{n2} is reached, sliding is resumed; however, I_{n2}, I_{t2} and I_{s2} cannot be obtained by the integration of (34a)–(34e), which become singular ($s(t =$

$t_S) = 0 \Rightarrow h(\mu, \hat{\phi}) = 0$). One way to navigate the solution through this singularity (see [9]) for $t > t_S$ is to let ϕ switch values from $\phi = \hat{\phi}$ to $\phi = \hat{\phi}$, the only solution of $h(\mu, \phi) = 0$ satisfying $ds/dI_n = g(\mu, \hat{\phi}) > 0$ (see Appendix B). If, in addition, $d\phi/dI_n = 0$ is imposed, then ϕ remains constant ($= \hat{\phi}$), $ds/dI_n = \text{const} = g(\mu, \hat{\phi}) > 0$ (see (34a) and (34b)), and, for $t_S < t \leq t_2$ (34a)–(34e) can be replaced with

$$d\phi/dI_n = 0, \tag{46a}$$

$$ds/dI_n = g(\mu, \hat{\phi}), \tag{46b}$$

$$dv_n/dI_n = f(\mu, \hat{\phi}), \tag{46c}$$

$$dI_t/dI_n = -\mu c \hat{\phi}, \tag{46d}$$

$$dI_s/dI_n = -\mu s \hat{\phi}. \tag{46e}$$

In conclusion, solutions to the 3D collision problem can be obtained by the integration of (34a)–(34e). If $s(t = t_S) = 0$, then (34a)–(34e) are replaced by either (45a)–(45e) or (46a)–(46e), according to whether $\mu > \mu_c$ (sticking) or $\mu < \mu_c$ (sliding renewal).

It may occur that $\mu = \mu_s \hat{=} m_{ns}/m_{ts}$; then initially $h(\mu, 0) = m_{ns} - \mu m_{ts} = 0$. In that event $\phi \equiv 0$, and the hodograph remains on the v_t axis unless sticking occurs with $\mu_s < \mu_c$; then sliding is renewed in the $\hat{\phi}$ direction. If $\mu_s > \mu_c$, sticking prevails.

Next, the assumption that I_{n2} is known is abandoned in favor of collision hypotheses which govern the integration limits. Accordingly, Newton’s [13], Poisson’s [14] and Stronge’s [11] collision hypotheses will be introduced, along with the following assumption, namely, that the collision time comprises a compression phase, starting at t_1 and terminating at t_C , the instant of maximum compression, when the normal relative velocity vanishes, i.e.,

$$v_{nC} \hat{=} \mathbf{v}^R(t_C) \cdot \mathbf{n} = 0 \quad (t_1 < t_C < t_2); \tag{47}$$

and a restitution phase, starting at t_C and terminating at t_2 , when $\mathbf{R}(t_2) = 0$ (see (5)).

4 Newton’s, Poisson’s and Stronge’s hypotheses

4.1 Newton’s hypothesis

In accordance with Newton’s hypothesis, the coefficient of restitution is defined

$$e \hat{=} -v_{n2}/v_{n1} \quad (0 \leq e \leq 1). \tag{48}$$

Here, the integration proceeds until $v_n = v_{n2}$.

4.2 Poisson’s hypothesis

Let I_{nC} and I_{nR} be parts of I_{n2} associated with the compression and with the restitution phases, respectively; then (see (10a))

$$I_{n2} = I_{nC} + I_{nR}, \quad I_{nC} \hat{=} \left(\int_{t_1}^{t_C} \mathbf{R} dt \right) \cdot \mathbf{n}, \quad I_{nR} \hat{=} \left(\int_{t_C}^{t_2} \mathbf{R} dt \right) \cdot \mathbf{n}. \tag{49}$$

According to Poisson’s hypothesis, the coefficient of restitution is defined

$$e \hat{=} I_{nR}/I_{nC} \quad (0 \leq e \leq 1), \tag{50}$$

so that, in light of (49) and (50)

$$I_{n2} = (1 + e)I_{nC}. \tag{51}$$

Here I_{nC} is recorded for which v_n vanishes. I_{n2} is then evaluated with (51), and the integration proceeds until $I_n = I_{n2}$.

4.3 Stronge’s hypothesis

Let $\Delta E_{nC} (< 0)$ and $\Delta E_{nR} (> 0)$ be parts of the ‘normal’ energy loss ΔE_{n2} (see (35b)) associated with the compression and the restitution phases, respectively; then

$$\Delta E_{n2} = \Delta E_{nC} + \Delta E_{nR}, \quad \Delta E_{nC} \hat{=} \int_0^{I_{nC}} v_n dI_n, \quad \Delta E_{nR} \hat{=} \int_{I_{nC}}^{I_{n2}} v_n dI_n. \tag{52}$$

According to Stronge’s hypothesis, the coefficient of restitution is defined

$$e^2 \hat{=} - \Delta E_{nR} / \Delta E_{nC} \quad (0 \leq e \leq 1), \tag{53}$$

so that, in light of (52) and (53)

$$\Delta E_{n2} = (1 - e^2)\Delta E_{nC}. \tag{54}$$

Here ΔE_{nC} is recorded for which v_n vanishes (see (35b)). ΔE_{n2} is then evaluated with (54), and the integration proceeds until $\Delta E_n = \Delta E_{n2}$.

The steps underlying the solution by integration can be summarized as follows:

1. Find \mathbf{n} , \mathbf{t} and \mathbf{s} satisfying relations (7b)–(7d), and identify \mathbf{V}_n , \mathbf{V}_t and \mathbf{V}_s ((12a)–(12d)), the members of \mathbf{M} ((9)) and \mathfrak{M} ((18)), c_n , c_t and c_s (41a)–(41c), and μ_c , ϕ_c ((43)); and $\hat{\phi}$ satisfying $h(\mu, \hat{\phi}) = 0$ with $g(\mu, \hat{\phi}) > 0$.
2. Introduce λ , a parameter, and integrate both sides of the expressions

$$[\text{Eqs.}(34i)](1 - |\lambda|) + [\text{Eqs.}(45i)]\lambda(\lambda - 1)/2 + [\text{Eqs.}(46i)]\lambda(\lambda + 1)/2 \tag{55}$$

with i playing the roles of a, b, c, d and e, one at a time, and with $\lambda(0) = 0$, $\phi(0) = 0$, $s(0) = v_{t1}$, $v_n(0) = v_{n1}$, $I_t(0) = 0$ and $I_s(0) = 0$ as initial conditions, switching, if $s < \varepsilon_s$, from the initial sliding ($\lambda = 0$) to sticking ($\mu > \mu_c$, $\lambda = -1$) or to sliding renewal ($\mu < \mu_c$, $\lambda = 1$). It can be shown that, if ε_s is sufficiently small, it has no effect on the integration results.

3. Identify v_{n2} , I_{n2} or ΔE_{n2} , and stop the integration according to the chosen collision hypothesis; find I_{n2} , I_{t2} and I_{s2} and then $\Delta u_1, \dots, \Delta u_p$ with (12a).
4. Evaluate the mechanical energy loss with both (23) (two versions) and (35a). Identical results validate of the entire procedure.

These steps need modifications, discussed in Appendix C, when used to solve the 2D problem. With these modifications, *all* the results reported in Table 3 of [3] for the planar version of the two-sled problem are reproduced with a three-digit precision.

5 The two-sled example ([30], p. 9)

Figure 2 shows two identical sleds A and B comprising rods of length $2l$ and mass m , supported by massless knife-edges with steering angles γ and δ , touching planes \bar{A} and

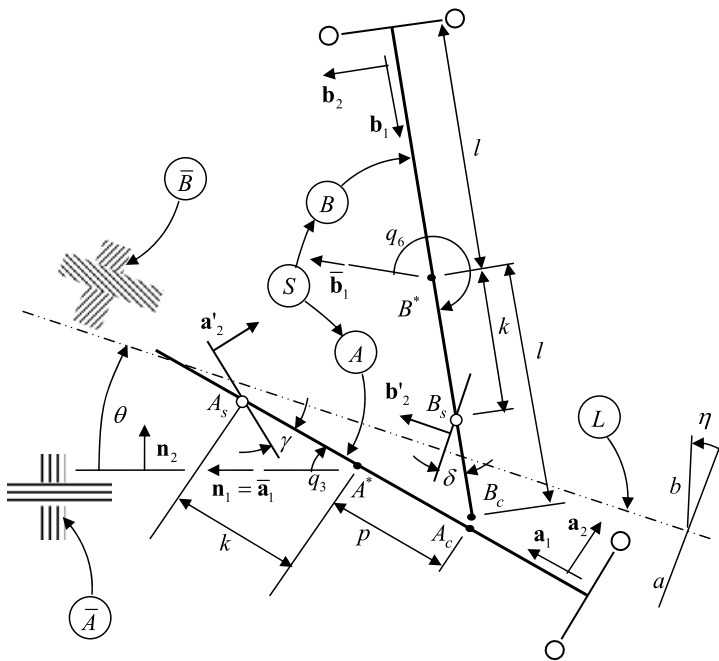


Fig. 2 A two-sled collision

\bar{B} fixed in N at points A_s and B_s , a distance k from their mass centers A^* and B^* ; and supported by two back sliders moving in \bar{A} and \bar{B} , respectively. \bar{A} and \bar{B} are rotated with respect to one another about their intersection line L forming an angle $\theta < \pi/2$ with $\bar{\mathbf{a}}_1$, a unit vector fixed in \bar{A} , such that lines a and b lying in \bar{A} and \bar{B} normal to L form an angle $\eta < \pi/2$; and $\bar{\mathbf{b}}_1|_{\eta=0} = \bar{\mathbf{a}}_1$. Let u_1, \dots, u_6 be generalized speeds, and let the velocities of A^* and B^* , and the angular velocities of A and B in N , expressed as

$$\mathbf{v}^{A^*} = u_1 \mathbf{a}_1 + u_2 \mathbf{a}_2, \quad \omega^A = u_3 \mathbf{a}_3, \quad \mathbf{v}^{B^*} = u_4 \mathbf{b}_1 + u_5 \mathbf{b}_2, \quad \omega^B = u_6 \mathbf{b}_3,$$

be subject to the constraints $\mathbf{v}^{A_s} \cdot \mathbf{a}'_2 = 0$ and $\mathbf{v}^{B_s} \cdot \mathbf{b}'_2 = 0$ imposed by the knife-edges. Here $\mathbf{a}_i, \mathbf{b}_i, \mathbf{a}'_i$ and \mathbf{b}'_i ($i = 1, 2, 3$) are sets of three dextral, mutually perpendicular unit vectors fixed in A and B , with \mathbf{a}_3 and \mathbf{a}'_3 , and \mathbf{b}_3 and \mathbf{b}'_3 normal to \bar{A} and \bar{B} , respectively, as shown in Fig. 2. The indicated constraint equations, when written explicitly and solved for u_2 and u_5 , read

$$u_2 = t\gamma u_1 - ku_3, \quad u_5 = t\delta u_4 - ku_6,$$

where $t(\cdot) = \tan(\cdot)$, and lead, with u_1, u_3, u_4 , and u_6 regarded as independent generalized speeds, to the following equations, governing motions of A and B :

$$\begin{aligned} -\dot{u}_1/c^2\gamma + kt\gamma\dot{u}_3 - ku_3^2 &= 0, & kt\gamma\dot{u}_1 - (l^2/3 + k^2)\dot{u}_3 + ku_1u_3 &= 0, \\ -\dot{u}_4/c^2\delta + kt\delta\dot{u}_6 - ku_6^2 &= 0, & kt\delta\dot{u}_4 - (l^2/3 + k^2)\dot{u}_6 + ku_4u_6 &= 0, \end{aligned}$$

where $s(\cdot) = \sin(\cdot)$ and $c(\cdot) = \cos(\cdot)$. Defining generalized coordinates q_1, \dots, q_6 as $q_1 \hat{=} \mathbf{p}^{A^*} \cdot \mathbf{a}_1, q_2 \hat{=} \mathbf{p}^{A^*} \cdot \mathbf{a}_2, \dot{q}_3 \hat{=} u_3$ and $q_4 \hat{=} \mathbf{p}^{B^*} \cdot \mathbf{b}_1, q_5 \hat{=} \mathbf{p}^{B^*} \cdot \mathbf{b}_2, \dot{q}_6 \hat{=} u_6$, one can replace

the constraint equations with

$$\begin{aligned}
 -s(\gamma + q_3)\dot{q}_1 + c(\gamma + q_3)\dot{q}_2 + kc\gamma\dot{q}_3 &= 0, \\
 -s(\delta + q_6)\dot{q}_4 + c(\delta + q_6)\dot{q}_5 + kc\delta\dot{q}_6 &= 0,
 \end{aligned}$$

non-integrable differential equations, which make the system non-holonomic. Next, suppose that at time t_1 the endpoint B_c of B collides with point A_c of A located a distance p from A^* ; and that it is required to evaluate the associated changes in the generalized speeds and in the system kinetic energy. To this end, the velocities of A_c and B_c are expressed as

$$\mathbf{v}^{A_c} = u_1\mathbf{a}_1 + (u_2 + pu_3)\mathbf{a}_2, \quad \mathbf{v}^{B_c} = u_4\mathbf{b}_1 + (u_5 + lu_6)\mathbf{b}_2,$$

and the relative velocity $\mathbf{v}^R = \mathbf{v}^{B_c} - \mathbf{v}^{A_c}$ of the colliding points is written, with $z_1 = (k - p)u_3 - t\gamma u_1$, $z_2 = (l - k)u_6 + t\delta u_4$, $z_3 = c\eta + c^2\theta(1 - c\eta)$, $z_4 = c\eta + s^2\theta(1 - c\eta)$, $z_5 = s\theta c\theta(1 - c\eta)$, $z_6 = z_5s q_6 + z_3c q_6$, $z_7 = z_5c q_6 - z_3s q_6$, $z_8 = z_5c q_6 + z_4s q_6$, and $z_9 = z_5s q_6 - z_4c q_6$, as

$$\begin{aligned}
 \mathbf{v}^R &= [(sq_3z_8 + cq_3z_6)u_4 - u_1 + (sq_3z_9 - cq_3z_7)z_2]\mathbf{a}_1 + [z_1 - (sq_3z_7 \\
 &+ cq_3z_9)z_2 - (sq_3z_6 - cq_3z_8)u_4]\mathbf{a}_2 + [c(\theta - q_6)z_2 - s(\theta - q_6)u_4]s\eta\mathbf{a}_3.
 \end{aligned}$$

With \mathbf{n} , \mathbf{t} and \mathbf{s} identified as $\mathbf{n} = \mathbf{a}_2$, $\mathbf{t} = c\varphi\mathbf{a}_1 + s\varphi\mathbf{a}_3$ and $\mathbf{s} = -s\varphi\mathbf{a}_1 + c\varphi\mathbf{a}_3$, φ can be found that satisfies $\mathbf{v}^R \cdot \mathbf{t} = v_{t1} > 0$ and $\mathbf{v}^R \cdot \mathbf{s} = v_{s1} = 0$, enabling the evaluation of \mathbf{V}_n , \mathbf{V}_t and \mathbf{V}_s ((12a)–(12d)) and of the members of \mathfrak{M} ((15)). With $m = 3$ kg, $l = 1$, $k = 0.75$, $p = -0.5m$, $\gamma = \delta = 0.2$, $\theta = \pi/3$, $\eta = 2\pi/9$ rad, $q_3(t_1) = \pi/4$, and $q_6(t_1) = 7\pi/4$ rad one can show, by substitutions, that $\varphi = 3.81$, $m_{nn} = 0.225$, $m_{tt} = 0.236$, $m_{ss} = 0.270$, $m_{nt} = -0.109$, $m_{ts} = -0.116$, $m_{ns} = -0.126$ ((18)), $c_n = 42.6$, $c_t = 37.3$, $c_s = 35.8$ ((41a)–(41c)), $\mu_c = 1.21$, $\phi_c = 3.76$ ((43)) and $\hat{\phi} = 3.91$ (Sect. 3.3). For $u_1(t_1) = u_4(t_1) = 1$ m/sec, $u_3(t_1) = u_6(t_1) = 0.1$ rad/sec ($v_{n1} = -0.9$, $v_{t1} = 1.06$, $v_{s1} = 0$ m/sec), one obtains, integrating (34a)–(34e), (45a)–(45e) and (46a)–(46e) with $\varepsilon_s = 0.1 \div 0.01$, results recorded in Table 1 and Fig. 3 for $\mu = 0.6, 1.1, 1.6$ and $e = 0.8$, where ‘○’, ‘+’ and ‘□’ designate collision termination points according Newton’s, Poisson’s and Stronge’s hypotheses, respectively. One can thus follow the hodographs as μ increases. For $\mu < \mu_s \hat{=} m_{ns}/m_{ts} = 1.086$ (e.g., $\mu = 0.6$) there is sliding, with a local maximum approaching the origin. If $\mu = \mu_s \Rightarrow h = 0$ (see end of Sect. 3.3) then $\phi \equiv 0$ throughout sliding ((34a)). The sliding part runs along the v_t axis, and is followed by a sliding renewal part. The latter becomes ‘shorter’ as μ increases toward μ_c , vanishing for $\mu = \mu_c$. For $\mu > \mu_c$ sliding is followed by sticking for all collision hypotheses; then the three hodograph end-points overlap at the origin. The similarity between the hodographs for the sliding and the sliding renewal cases corroborates the ‘switch’ between $\bar{\phi}$ and $\hat{\phi}$ when sliding renewal occurs (Appendix B). Regarding energy gains associated with Newton’s hypothesis, it turns out to be significantly larger than that recorded for 2D systems, e.g. in [17] and [28].

It may occur that the number of collisions become large, as when numerous particles or bodies collide with one another. In that case the use of elaborate numerical integrators to solve (55) can produce prohibitively long simulations, unless exact integrals exist, e.g., when $\mu = 0$ ([5] and [6]) or when $m_{nt} = m_{ns} = m_{ts} = 0$. This state of affairs can be alleviated with recursive summation-based solutions, which, taking advantage of the limited integration range of (55), provide a reasonable compromise between accuracy and speed. Such a solution is discussed next.

Table 1 Changes of the motion variables and of the system energy for the example

μ	Newton's hypothesis		Poisson's hypothesis		Stronge's hypothesis	
	$[\Delta u_1, \Delta u_3, \Delta u_4, \Delta u_6]$	ΔE	$[\Delta u_1, \Delta u_3, \Delta u_4, \Delta u_6]$	ΔE	$[\Delta u_1, \Delta u_3, \Delta u_4, \Delta u_6]$	ΔE
0.6	$[-1.13, 0.64, -1.71, -0.03]$	-1.44	$[-1.05, 0.39, -1.35, -0.01]$	-2.49	$[-1.07, 0.47, -1.46, -0.01]$	-2.23
1.1	$[-1.04, 1.63, -1.41, 0.12]$	+1.37	$[-0.98, 0.29, -1.06, 0.05]$	-2.82	$[-0.99, 0.58, -1.13, 0.07]$	-2.38
1.6	$[-0.90, 2.90, -1.03, 0.30]$	+9.16	$[-0.96, 0.21, -1.01, 0.05]$	-2.90	$[-0.96, 0.63, -1.01, 0.09]$	-2.31

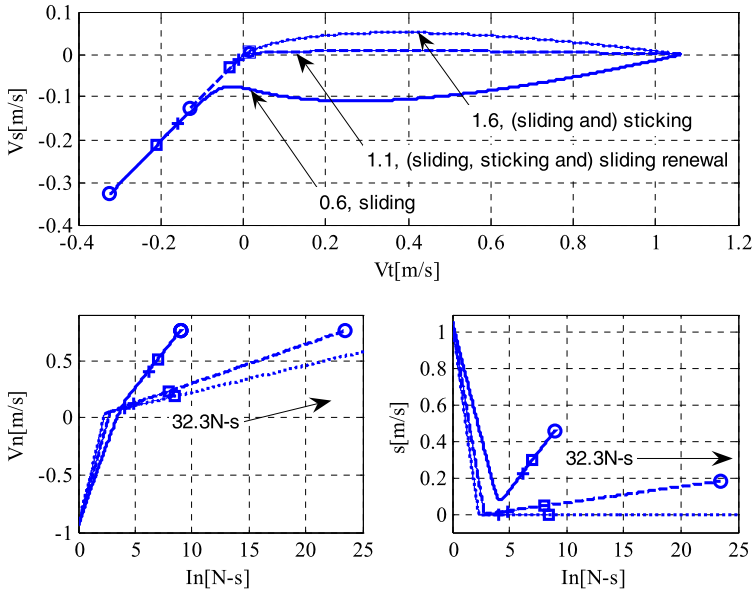


Fig. 3 v_s vs. v_t (hodograph) and v_n and s vs. I_n for $\mu = 0.6, 1.1, 1.6$, yielding sliding, sliding renewal ($\hat{\phi} = 0.432$) and sticking ($\hat{\phi} = 0.598$), respectively

6 Solution by recursive summation

6.1 Recursive summation

Referring to Euler’s explicit, first order accurate method, described, e.g., in [31], Para. 3, Sect. 9, let $I_n(1) = 0, I_n(i) = (i - 1)/k, D(i) \hat{=} I_n(i) - I_n(i - 1) (i = 2, 3, \dots)$, where k , an integer, is a refinement factor, and replace (55) with

$$\phi(i) \stackrel{(34a), (45a), (46a)}{=} \{ \phi(i - 1) + [h(i - 1)/s(i - 1)]D(i) \} (1 - |\lambda|) + \hat{\phi} \lambda (\lambda + 1)/2, \tag{56a}$$

$$f(i) \stackrel{(31)}{=} m_{nn} - \mu m_{nt} c \phi(i) - \mu m_{ns} s \phi(i), \tag{56b}$$

$$g(i) \stackrel{(32)}{=} m_{nt} c \phi(i) + m_{ns} s \phi(i) - \mu m_{tt} c^2 \phi(i) - \mu m_{ss} s^2 \phi(i) - 2 \mu m_{ts} s \phi(i) c \phi(i), \tag{56c}$$

$$h(i) \stackrel{(33)}{=} -m_{nt} s \phi(i) + m_{ns} c \phi(i) - \mu m_{ts} [c^2 \phi(i) - s^2 \phi(i)] + \mu (m_{tt} - m_{ss}) s \phi(i) c \phi(i), \tag{56d}$$

$$s(i) \stackrel{(34b), (45b), (46b)}{=} [s(i - 1) + g(i - 1)D(i)] [1 - |\lambda| + \lambda(\lambda + 1)/2], \tag{56e}$$

$$\begin{aligned} v_n(i) \stackrel{(34c), (45c), (46c)}{=} & [v_n(i - 1) + f(i)D(i)] (1 - |\lambda|) \\ & + v_n(i - 1)D(i) \hat{f} [\lambda(\lambda + 1)/2] \\ & + v_n(i - 1)D(i)/c_n [\lambda(\lambda - 1)/2], \end{aligned} \tag{56f}$$

$$\begin{aligned}
 I_t(i) &\stackrel{(34d),(45d),(46d)}{=} [I_t(i-1) - \mu c \phi(i) D(i)](1 - |\lambda|) \\
 &\quad + [I_t(i-1) - \mu c \hat{\phi} D(i)] [\lambda(\lambda + 1)/2] \\
 &\quad + [I_t(i-1) + c_t/c_n D(i)] [\lambda(\lambda - 1)/2], \tag{56g}
 \end{aligned}$$

$$\begin{aligned}
 I_s(i) &\stackrel{(34e),(45e),(46e)}{=} [I_t(i-1) - \mu s \phi(i) D(i)](1 - |\lambda|) \\
 &\quad + [I_s(i-1) - \mu s \hat{\phi} D(i)] [\lambda(\lambda + 1)/2] \\
 &\quad + [I_s(i-1) + c_s/c_n D(i)] [\lambda(\lambda - 1)/2], \tag{56h}
 \end{aligned}$$

$$v_t(i) \stackrel{(28a)}{=} s(i) c \phi(i), \tag{56i}$$

$$v_s(i) \stackrel{(28c)}{=} s(i) s \phi(i), \tag{56j}$$

$$\Delta E(i) \stackrel{(35a)}{=} \Delta E(i-1) + [v_n(i) - \mu s(i)] D(i), \tag{56k}$$

$$\Delta E_n(i) \stackrel{(35b)}{=} \Delta E_n(i-1) + v_n(i) D(i), \tag{56l}$$

where $\lambda = 0$, $\phi(1) = 0$, $s(1) = v_{t1}$, $v_n(1) = v_{n1}$, $I_t(1) = I_s(1) = \Delta E(1) = \Delta E_n(1) = 0$, and $f(1) = m_{nn} - \mu m_{nt}$, $g(1) = m_{nt} - \mu m_{tt}$, $h(1) = m_{ns} - \mu m_{ts}$. Now, by [31] Euler’s method is stable if each of the eigenvectors $\lambda_j (j = 1, \dots, 5)$ of the coefficient matrix of the linearized right-hand-sides of (34a)–(34e) about a point $\phi_0, s_0, v_{n0}, I_{t0}$ and I_{s0} ‘close’ to the integration range satisfies the inequalities $|1 - \lambda_j D| \leq 1$, $D = D(i)/k$ being the summation step. There are two nonzero eigenvector associated with (34a)–(34e), namely $\lambda_{1,2} = 1/s_0 (h'_0 \pm \sqrt{h_0'^2 - 4h_0 g'_0})$, $h'_0 \hat{=} dh/d\phi|_{\phi=\phi_0}$, $g'_0 \hat{=} dg/d\phi|_{\phi=\phi_0}$, drifting apart as $s_0 \rightarrow 0$, thus leading to a stiffer system. At the limit $s_0 = 0$, hence (Sect. 3.2) $h_0 = h(\bar{\phi}) = 0$ ($\phi_0 = \bar{\phi}$). Only one nonzero, infinitely large eigenvector remains, which decrees $0 < h'_0/s_0 D < 1$, and, with a finite summation step, leads to instability accompanied by relatively poor results. One obtains for $D(i) = 1, k = 1$ (i.e., 5-8 summation steps) a ~96% agreement with the results of Sect. 5 for $\mu = 0.6$, and (only) ~70% agreement for $\mu = 1.1, 1.6$, where $s_0 = 0$ (sticking) is reached. Increasing k to 5, one has ~98% and ~90% agreement, respectively. Further investigation of this procedure is left for future work.

6.2 Partial integration/recursive summation (i/rs)

Equations (45a)–(45e) and (46a)–(46e) can be integrated analytically. Thus, a one-step evaluation can replace integration or recursive summation for the sticking or the sliding renewal parts of the collision, saving computation time. To show this, suppose again that the normal impulse I_{n2} is known. If, in the i/rs process, I_{n2} is reached with $s > 0$, then sliding prevails. If, however, s vanishes before I_{n2} is reached, then the associated values of v_n, I_n, I_t and I_s , denoted v_{nS}, I_{nS}, I_{tS} and I_{sS} , obtained with (34a)–(34e) or (56a)–(56l) (for $\lambda = 0$) are recorded, and used to identify $v_{n2}, I_{n2}, I_{t2}, I_{s2}$ and ΔE_{n2} , as follows. If $\mu > \mu_c$, then sticking prevails, and I_{n2}, I_{t2} and I_{s2} can be obtained by the analytic integration of (45a)–(45e) from t_S to t_C and from t_C to t_2 if $t_C > t_S$ (sticking in compression), yielding

$$I_{nC} \stackrel{(45c)}{=} I_{nS} + c_n(0 - v_{nS}), \tag{57a}$$

$$I_{n2} \stackrel{(45c)}{=} I_{nC} + c_n(v_{n2} - 0), \tag{57b}$$

$$I_{tC} \stackrel{(45c,d)}{=} I_{tS} + c_t(0 - v_{nS}), \tag{57c}$$

$$I_{t2} \stackrel{(45c,d)}{=} I_{tC} + c_t(v_{n2} - 0), \tag{57d}$$

$$I_{sC} \stackrel{(45c,e)}{=} I_{sS} + c_s(0 - v_{nS}), \tag{57e}$$

$$I_{s2} \stackrel{(45c,e)}{=} I_{sC} + c_s(v_{n2} - 0), \tag{57f}$$

where (47) was used; or from t_S to t_2 if $t_C < t_S$ (sticking in restitution), yielding

$$I_{n2} \stackrel{(45c)}{=} I_{nS} + c_n(v_{n2} - v_{nS}), \tag{58a}$$

$$I_{t2} \stackrel{(45c,d)}{=} I_{tS} + c_t(v_{n2} - v_{nS}), \tag{58b}$$

$$I_{s2} \stackrel{(45c,e)}{=} I_{sS} + c_s(v_{n2} - v_{nS}), \tag{58c}$$

relations valid also for sticking in compression. If, on the other hand, $\mu < \mu_c$, then sliding renewal prevails, and I_{n2} , I_{t2} and I_{s2} can be obtained by the analytic integration of (46a)–(46e) from t_S to t_C and from t_C to t_2 if $t_C > t_S$ (sliding renewal in compression), yielding

$$I_{nC} \stackrel{(46c)}{=} I_{nS} + (1/\hat{f})(0 - v_{nS}), \tag{59a}$$

$$I_{n2} \stackrel{(46c)}{=} I_{nC} + (1/\hat{f})(v_{n2} - 0), \tag{59b}$$

$$I_{tC} \stackrel{(46c,d)}{=} I_{tS} - (\mu c \hat{\phi} / \hat{f})(0 - v_{nS}), \tag{59c}$$

$$I_{t2} \stackrel{(46c,d)}{=} I_{tC} - (\mu c \hat{\phi} / \hat{f})(v_{n2} - 0), \tag{59d}$$

$$I_{sC} \stackrel{(46c,e)}{=} I_{sS} - (\mu s \hat{\phi} / \hat{f})(0 - v_{nS}), \tag{59e}$$

$$I_{s2} \stackrel{(46c,e)}{=} I_{sC} - (\mu s \hat{\phi} / \hat{f})(v_{n2} - 0), \tag{59f}$$

$$v_{tC} \stackrel{(36a)}{=} (\hat{g} c \hat{\phi} / \hat{f})(0 - v_{nS}), \tag{59g}$$

$$v_{t2} \stackrel{(36a)}{=} v_{tC} + (\hat{g} c \hat{\phi} / \hat{f})(v_{n2} - 0), \tag{59h}$$

$$v_{sC} \stackrel{(36b)}{=} (\hat{g} s \hat{\phi} / \hat{f})(0 - v_{nS}), \tag{59i}$$

$$v_{s2} \stackrel{(36b)}{=} v_{sC} + (\hat{g} s \hat{\phi} / \hat{f})(v_{n2} - 0), \tag{59j}$$

where (47) was used with $\hat{f} \stackrel{(31)}{\hat{=}} f(\mu, \hat{\phi})$ and $\hat{g} \stackrel{(32)}{\hat{=}} g(\mu, \hat{\phi})$; or from t_S to t_2 if $t_C < t_S$ (sliding renewal in restitution), yielding

$$I_{n2} \stackrel{(46c)}{=} I_{nS} + (1/\hat{f})(v_{n2} - v_{nS}), \tag{60a}$$

$$I_{t2} \stackrel{(46c,d)}{=} I_{tS} - (\mu c \hat{\phi} / \hat{f})(v_{n2} - v_{nS}), \tag{60b}$$

$$I_{s2} \underset{(46c,e)}{=} I_{sS} - (\mu s \hat{\phi} / \hat{f})(v_{n2} - v_{nS}), \tag{60c}$$

$$v_{r2} \underset{(36a)}{=} (\hat{g}c\hat{\phi} / \hat{f})(v_{n2} - v_{nS}), \tag{60d}$$

$$v_{s2} \underset{(36b)}{=} (\hat{g}s\hat{\phi} / \hat{f})(v_{n2} - v_{nS}), \tag{60e}$$

relations valid also for sliding renewal in compression.

The use of (57a)–(57f) and (60a)–(60e) can limit the integration or the recursive summation to the sliding part of the collision with the aid of the following collision hypothesis-dependent procedures, all starting with the evaluation of s , v_n , I_n , I_t and I_s by i/rs.

6.3 Collision hypotheses

6.3.1 Newton’s hypothesis

If, during i/rs, v_{n2} is reached with $s(v_{n2}) > 0$, then $I_{n2} = I_n(v_n = v_{n2})$, $I_{t2} = I_t(v_n = v_{n2})$ and $I_{s2} = I_s(v_n = v_{n2})$ are identified. If $s(v_n < v_{n2}) = 0$, then v_{nS} , I_{nS} , I_{tS} and I_{sS} are recorded, and used to evaluate I_{n2} , I_{t2} and I_{s2} either with (58a)–(58c) or with (60a)–(60c), depending on whether $\mu > \mu_c$ (sticking) or $\mu < \mu_c$ (sliding renewal), respectively.

6.3.2 Poisson’s hypothesis

If, during i/rs, $v_n = 0$ occurs before s vanishes ($t_C < t_S$), then I_{nC} is recorded, and I_{n2} calculated ((51)). The i/rs proceeds until $s = 0$ or $I_n = I_{n2}$. If $I_n = I_{n2}$ occurs first, then sliding prevails, and I_{n2} , $I_{t2} = I_t(I_n = I_{n2})$ and $I_{s2} = I_s(I_n = I_{n2})$ are identified during the i/rs. If $s = 0$ occurs first, then v_{nS} , I_{nS} , I_{tS} and I_{sS} are recorded. If $\mu > \mu_c$, then sticking prevails in restitution, and v_{n2} , and then I_{t2} and I_{s2} are evaluated with (58a), and then (58b) and (58c), respectively. If $\mu < \mu_c$, then sliding renewal prevails in restitution, and v_{n2} , and then I_{t2} and I_{s2} are evaluated with (60a), and then (60b) and (60c), respectively. Next, if $s = 0$ occurs before $v_n = 0$ ($t_C > t_S$), then v_{nS} , I_{nS} , I_{tS} and I_{sS} are recorded. If $\mu > \mu_c$, then sticking prevails in compression. I_{nC} and I_{n2} are obtained from (57a) and (51); and v_{n2} , and then I_{t2} and I_{s2} are evaluated with (58a), and then (58b) and (58c), respectively. Finally, if $\mu < \mu_c$, then sliding renewal prevails in compression. I_{nC} and I_{n2} are obtained from (59a) and (51); and v_{n2} , and then I_{t2} and I_{s2} are evaluated with (60a), and then (60b) and (60c), respectively.

6.3.3 Stronge’s hypothesis

Here ΔE_n is obtained by i/rs (see (35b)/(56l)) as well. If $v_n = 0$ occurs before s vanishes ($t_C < t_S$, $I_{nC} < I_{nS}$), then ΔE_{nC} is recorded, and ΔE_{n2} is evaluated ((54)). The i/rs proceeds until $s = 0$ or ΔE_{n2} is reached. If ΔE_{n2} is reached first, then sliding prevails, and $I_{n2} = I_n(\Delta E_n = \Delta E_{n2})$, $I_{t2} = I_t(\Delta E_n = \Delta E_{n2})$ and $I_{s2} = I_s(\Delta E_n = \Delta E_{n2})$ are identified during the i/rs. If $s = 0$ occurs first, then v_{nS} , I_{nS} , I_{tS} , I_{sS} and ΔE_{nS} are recorded. Now, if $\mu > \mu_c$, then sticking prevails in restitution, and one can write $\Delta E_{n2} - \Delta E_{nS} \underset{(35b)}{=} \int_{I_{nS}}^{I_{n2}} v_n dI_n \underset{(45c)}{=} c_n \int_{v_{nS}}^{v_{n2}} v_n dv_n = c_n(v_{n2}^2 - v_{nS}^2)/2$, which yields

$$v_{n2} = \{v_{nS}^2 + 2/c_n[(1 - e^2)\Delta E_{nC} - \Delta E_{nS}]\}^{1/2}, \tag{61}$$

in accordance with (54). The positive root was chosen to ensure $v_{n2} > 0$ and $\partial v_{n2}/\partial e > 0$; and I_{n2} , I_{t2} and I_{s2} are evaluated with (58a)–(58c). If $\mu < \mu_c$, then sliding renewal prevails in restitution, v_{n2} is evaluated by (61) with $1/\hat{f}$ replacing c_n ($dv_n/dI_n \stackrel{(46c)}{=} \hat{f}[\hat{=} f(\mu, \hat{\phi})]$) replaces $dv_n/dI_n \stackrel{(45c)}{=} 1/c_n$); and I_{n2} , I_{t2} and I_{s2} are evaluated with (60a)–(60c). Next, if $s = 0$ occurs while $v_n < 0$ ($t_C > t_S$, $I_{nC} > I_{nS}$), then v_{nS} , I_{nS} , I_{tS} , I_{sS} and ΔE_{nS} are recorded. If $\mu > \mu_c$, then sticking prevails in compression, and $\Delta E_{nC} - \Delta E_{nS} \stackrel{(35b)}{=} \int_{I_{nS}}^{I_{nC}} v_n dI_n \stackrel{(45c)}{=} c_n \int_{v_{nS}}^{v_{nC}} v_n dv_n \stackrel{(47)}{=} -c_n v_{nS}^2/2$, or

$$\Delta E_{nC} = \Delta E_{nS} - c_n v_{nS}^2/2. \tag{62}$$

One can then obtain v_{n2} by substitution form (62) in (61), and then evaluate I_{n2} , I_{t2} and I_{s2} with (58a)–(58c). Finally, if $\mu < \mu_c$, then sliding renewal prevails in compression. ΔE_{nC} is identified with the aid of (62) with $1/\hat{f}$ replacing c_n . Then (61) is used to evaluate v_{n2} (again with $1/\hat{f}$ replacing c_n), which is then used to uncover I_{n2} , I_{t2} and I_{s2} with (60a)–(60c).

For the last two cases of Table 1 one obtains, integrating (34a)–(34e) in conjunction with (58a)–(58c), (60a)–(60c), (61) and (62),

$$\begin{aligned} \mu = 1.1 \quad \Rightarrow \quad \Delta E_{nC} = -1.295, \quad \Delta E_{nS} = -1.291, \\ \hat{f} = 0.0425, \quad v_{nS} = 0.0533 \quad \Rightarrow_{(61)} \quad v_{n2} = 0.203, \\ \\ \mu = 1.6 \quad \Rightarrow \quad \Delta E_{nC} = -1.085, \quad \Delta E_{nS} = -1.083, \\ c_n = 42.59, \quad v_{nS} = 0.0402 \quad \Rightarrow_{(61)} \quad v_{n2} = 0.267, \end{aligned}$$

the exact results (within four digits) obtained by the integration of (55).

7 Conclusions

Three sets of five differential equations governing 3D one-point collision with friction problems associated with simple, non-holonomic systems were discussed, and shown to possess unique solutions. Ways to speed up the integration were presented, whereby the integration of equations governing the sliding part of the collision was replaced with recursive summation, and the integration of equations governing the sticking and sliding renewal parts were replaced with a one-step evaluation of the impulse components. It was also demonstrated that Newton’s hypothesis can lead to energy discrepancy significantly exceeding the values recorded to-date for planar systems. Finally, it is noted that there is no clear cut proof that Poisson’s hypothesis always lead to energy-consistent solutions in 3D systems, leaving Stronge’s hypothesis the most suitable for the type of solution under consideration.

Appendix A

The kinetic energy of a system S of v particles described in Sect. 2 is given by $E = 1/2 \sum_{i=1}^v m_i (\mathbf{v}^i)^2$, a positive quantity which can be cast into the form

$$E = -1/2 \sum_{r=1}^p \sum_{s=1}^p m_{rs} u_r u_s = 1/2 \mathbf{u}(-\mathbf{M})\mathbf{u}^T > 0; \quad \mathbf{u} \hat{=} |u_1, \dots, u_p| \tag{63}$$

where $m_{rs} \hat{=} -\sum_{i=1}^v m_i \mathbf{v}_r^{P_i} \cdot \mathbf{v}_s^{P_i}$, if $\mathbf{v}_i^{P_i} = 0, i = 1, \dots, v$ (see (2)), rendering the mass matrix $-M$ symmetric and positive definite. Now, the coefficient matrix \mathfrak{M} of (23)–(25) is also positive definite. To show this, note that \mathfrak{M} can be written

$$\mathfrak{M} = \mathbf{V}(-\mathbf{M}^{-1})\mathbf{V}^T \tag{64}$$

where \mathbf{V} is $3 \times p$ matrix appearing in (14). Because $-\mathbf{M}$ hence $-\mathbf{M}^{-1}$ are positive definite matrices, one can write ([32], p. 109)

$$-\mathbf{M}^{-1} = \mathbf{A}\mathbf{A}^T = \mathbf{A}^T\mathbf{A}. \tag{65}$$

Thus,

$$\mathfrak{M} = \mathbf{V}\mathbf{A}\mathbf{A}^T\mathbf{V}^T = \mathbf{B}\mathbf{B}^T; \quad \mathbf{B} = \mathbf{V}\mathbf{A} \tag{66}$$

and, since $\det(\mathbf{B}\mathbf{B}^T) = \det \mathbf{B} \det \mathbf{B}^T = (\det \mathbf{B})^2 > 0$, then $\det \mathfrak{M} = \det(\mathbf{B}\mathbf{B}^T) > 0$, where

$$\det \mathfrak{M} = m_{nn}m_{ss}m_{tt} - (m_{nn}m_{ts}^2 + m_{tt}m_{ns}^2 + m_{ss}m_{nt}^2) + 2m_{nt}m_{ns}m_{ts} > 0. \tag{67}$$

By the same token, the removal of the first, second or third row of \mathbf{V} reduces $\mathbf{V}(-\mathbf{M}^{-1})\mathbf{V}^T$ to 2×2 diagonal submatrices of \mathfrak{M} , obtained by the removal of the first, second or third row-and-column of \mathfrak{M} , respectively. As with the 3×3 case, these submatrices have positive determinants, namely

$$m_{nn}m_{tt} - m_{nt}^2 > 0, \quad m_{nn}m_{ss} - m_{ns}^2 > 0, \quad m_{tt}m_{ss} - m_{ts}^2 > 0. \tag{68}$$

The removal of any two of the rows of \mathbf{V} reduces $\mathbf{V}(-\mathbf{M}^{-1})\mathbf{V}^T$ to one of the diagonal elements of \mathfrak{M} , positive numbers defined in the first, third and last of (15). Thus, the principal submatrices of \mathfrak{M} are all positive, hence \mathfrak{M} is positive definite ([32], p. 250).

Appendix B

If $g(\mu, \phi) = 0$ and $h(\mu, \phi) = 0$ (see (44)), then also $\mu g(\mu, \phi) = 0$ and $\mu h(\mu, \phi) = 0$; and these equations become, if the substitutions $u = \mu c\phi$ and $v = \mu s\phi$ are used,

$$\mu g \stackrel{(32)}{=} -m_{tt}u^2 - 2m_{ts}uv - m_{ss}v^2 + m_{nt}u + m_{ns}v = 0, \tag{69}$$

$$\mu h \stackrel{(33)}{=} m_{ts}u^2 - 2[(m_{tt} - m_{ss})/2]uv - m_{ts}v^2 - m_{ns}u + m_{nt}v = 0, \tag{70}$$

even and odd functions, respectively of v, m_{ns} and m_{ts} ($\mu g(v, m_{ns}, m_{ts}) = \mu g(-v, -m_{ns}, -m_{ts}) = 0$ and $\mu h(v, m_{ns}, m_{ts}) = -\mu h(-v, -m_{ns}, -m_{ts}) = 0$). The coordinate transformation $|u'v'| = |uv|\mathbf{T}$, where the columns of \mathbf{T} are the eigenvectors of the coefficient matrix $\mathbf{g} = |m_{tt}m_{ts}; m_{ts}m_{ss}|$, brings (69) into the form $\lambda_1 u'^2 + \lambda_2 v'^2 + (\)u' + (\)v' = 0$, where λ_1 and λ_2 are the eigenvalues of \mathbf{g} ([32], p. 255) given by

$$\lambda_{1,2} = \{(m_{tt} + m_{ss}) \pm [(m_{tt} + m_{ss})^2 - 4(m_{tt}m_{ss} - m_{ts}^2)]^{1/2}\}/2. \tag{71}$$

Here $\lambda_1 > 0$ and $\lambda_2 > 0$ (the expression under the root is always positive and smaller than $m_{tt} + m_{ss}$), therefore (69) represents an ellipse passing through the origin, as illustrated in

Fig. 4 The ellipse and the hyperbola for the example of Sect. 5, with circular segments designating $\mu = 0.6, 1.1, 1.6$ and $\mu_c = 1.21$

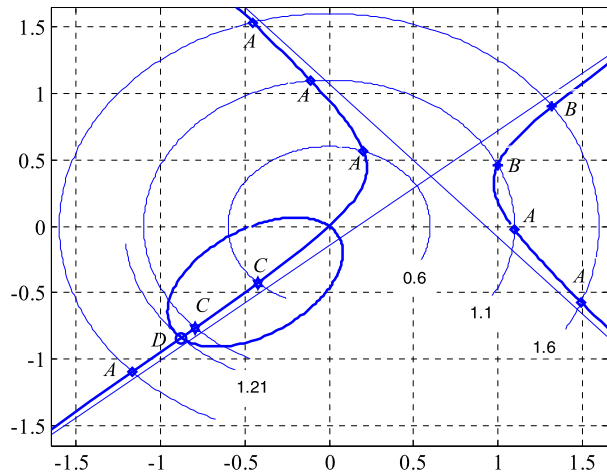


Fig. 4 for the example of Sect. 5. Similarly for (70), the eigenvalues of the coefficient matrix $\mathbf{h} = |m_{ts} - (m_{tt} - m_{ss})/2; -(m_{tt} - m_{ss})/2 - m_{ts}|$ are

$$\lambda_{1,2} = \pm \{m_{ts}^2 + [(m_{tt} - m_{ss})/2]^2\}^{1/2}, \tag{72}$$

and, since $\lambda_1 > 0$ and $\lambda_2 = -\lambda_1$, (70) represents a hyperbola with orthogonal asymptotes parallel to the lines $u' = \pm v'$. Its branches are called ‘remote’ and ‘near’, the latter passing through the origin (Fig. 4). The normalized (unit) eigenvectors of \mathbf{g} and \mathbf{h} are Sines and Cosines of ϕ_e and ϕ_h , uniquely determined angles describing the orientation of the major axes of the ellipse and the hyperbola with respect to the $u - v$ axes. ϕ_e and ϕ_h satisfy the relations

$$t(2\phi_e) = 2m_{ts}/(m_{tt} - m_{ss}), \quad t(2\phi_h) = -1/2(m_{tt} - m_{ss})/m_{ts}, \tag{73}$$

so that the angle between the major axes of the ellipse and the hyperbola is $\pi/4$ (see Fig 4). Moreover, the ellipse and the hyperbola intersect at the origin $u = v (= \mu) = 0$, where they are perpendicular, i.e.,

$$g(\mu, \phi)|_{\mu=0} = 0 \Rightarrow t\phi = -m_{nt}/m_{ns}; \quad h(\mu, \phi)|_{\mu=0} = 0 \Rightarrow t\phi = m_{ns}/m_{nt}; \tag{74}$$

and at point (μ_c, ϕ_c) described by (43) as a *unique* solution of (44) (or (69) and (70)), hence lie on the near branch of the hyperbola (so that the remote branch does not intersect the ellipse). Note that point $(0, 0)$ is not a solution of (44), for $g(0, 0) = m_{nt} \neq h(0, 0) = m_{ns}$ (see (32) and (33)). Now $g(\mu, \phi)$ can be written

$$g(\mu, \phi) = m_{nt}c\phi + m_{ns}s\phi + \mu[-|c\phi s\phi||m_{tt}m_{ts}; m_{ts}m_{ss}||c\phi s\phi|^T]. \tag{75}$$

The expression multiplying μ comprises a negative number (Appendix A, (68)). Consequently, if l is a line passing through the origin and point (μ_e, ϕ_e) on the ellipse ($g(\mu_e, \phi_e) = 0$), then the (cylindrical) coordinates μ and ϕ_e of points of l satisfy either $g(\mu, \phi_e) > 0$ or $g(\mu, \phi_e) < 0$, depending on whether the indicated point is inside ($\mu < \mu_e$) or outside ($\mu > \mu_e$) the ellipse. If a circle of radius μ is drawn with its center at the origin, then the orientation angles of lines passing through the origin and each of the intersection points of

the circle with the hyperbola (two or four), are solutions of $h(\mu, \phi) = 0$. If outside the ellipse, these points satisfy $g(\mu, \phi) < 0$ (e.g., Points *A* and *B* in Fig. 4). However, if $\mu < \mu_c$, then one, and only one of these points, namely $(\mu, \hat{\phi})$, lies within the ellipse (e.g., Points *C* in Fig. 4); and, because $g(\mu, \hat{\phi}) > 0$, it accommodates sliding renewal in direction $\hat{\phi}$ (Sect. 3.3). Points *B* accommodate angle $\bar{\phi}$ (Sect. 3.2) and Point *D* accommodates μ_c and ϕ_c ((43)).

Appendix C

In 2D systems

1. $m_{ns} = m_{ts} = m_{ss} = 0$, hence $c_n = c_t = c_s = 0$ (see (41a)–(41c)); and μ_c and ϕ_c (43) become undefined. With $\phi \equiv 0$ and $d\phi/dI_n = 0$ (34a)–(34e) remain intact.
2. Equations (25)–(27) reduce to $dv_n = \Delta/m_{nt}dI_n$, $dI_t = -m_{nt}/\Delta$, $dI_s = 0$ where $\Delta \triangleq m_{nn}m_{tt} - m_{nt}^2$, hence (45a)–(45e) become $d\phi/dI_n = 0$, $ds/dI_n = 0$, $dv_n/dI_n = \Delta/m_{tt}$, $dI_t/dI_n = -m_{nt}/m_{tt}$, $dI_s/dI_n = 0$.
3. The solution of $h(\mu, \phi) = 0$, $g(\mu, \phi) > 0$ is $\hat{\phi} = \pi$, leaving (46a)–(46e) intact.

The procedure of Sect. 4 can be applied to 2D systems if modified accordingly.

References

1. Chatterjee, A., Ruina, A.: A new algebraic rigid-body collision law based on impulse space consideration. *J. Appl. Mech.* **65**, 939–951 (1998)
2. Najafabadi, S.A.M., Kovacs, J., Angeles, J.: A comparative study of approaches to dynamics modeling of contact transitions in multibody systems. In: Proceedings of IDETC/CIE 2005 Conferences, DET2005-85418, Long Beach, CA, 24–28 Sep. 2005
3. Djerassi, S.: Stronge's hypothesis-based solution to the collision-with-friction problem. *Multibody Syst. Dyn.* **24**, 493–515 (2010). doi:10.1007/s11044-010-9200-4
4. Keller, J.B.: Impact with friction. *J. Appl. Mech.* **53**, 1–4 (1986)
5. Whittaker, E.T.: A Treatise on the Analytical Dynamics of Particles & Rigid Bodies. Cambridge University Press, Cambridge (1904) (reprint 1993)
6. Wang, D., Conti, C., Beale, D.: Interference impact of multibody systems. *J. Mech. Des.* **121**, 128–135 (1999)
7. Smith, C.E.: Predicting rebounds using rigid-body dynamics. *J. Appl. Mech.* **58**, 754–758 (1991)
8. Batlle, A.J.: Rough balanced collision. *J. Appl. Mech.* **63**, 168–172 (1996)
9. Bhatt, V., Koechling, J.: Three-dimensional frictional rigid-body impact. *J. Appl. Mech.* **62**, 893–898 (1995)
10. Battle, J.A.: The sliding velocities flow of rough collisions in multibody systems. *J. Appl. Mech.* **63**, 804–809 (1996)
11. Stronge, W.J.: Impact Mechanics. Cambridge University Press, Cambridge (2000)
12. Zhen, Z., Liu, C.: The Analysis and Simulation for three-dimensional impact with friction. *Multibody Syst. Dyn.* **18**, 511–530 (2007)
13. Newton, I.: Philosophias Naturalis Principia Mathematica. R. Soc. Press, London (1686)
14. Poisson, S.D.: Mechanics. Longmans, London (1817)
15. Boulanger, G.: Note sur le choc avec frottement des corps non parfaitement elastique. *Rev. Sci.* **77**, 325–327 (1939)
16. Najafabadi, S.A.M., Kovacs, J., Angeles, J.: Generalization of the energetic coefficient of restitution for contacts in multibody systems. *J. Comput. Nonlinear Dyn.* **3**, 041008 (2008)
17. Kane, T.R., Levinson, D.A.: Dynamics: Theory and Application. McGraw Hill, New York (1985)
18. Rubin, M.B.: Physical restrictions on the impulse acting during three-dimensional impact of two 'rigid' bodies. *J. Appl. Mech.* **65**, 464–469 (1998)
19. Ivanov, A.P.: Energetics of a collision with friction. *J. Appl. Math. Mech.* **56**(4), 527–534 (1992)
20. Brach, R.M.: Rigid body collisions. *J. Appl. Mech.* **56**, 133–138 (1989)

21. Routh, E.J.: *Dynamics of a System of Rigid Bodies. Elementary Part*, 7th edn. Dover, New York (1905)
22. Hurmuzlu, Y.: An energy-based coefficient of restitution for planar impacts of slender bars with massive external surface. *J. Appl. Mech.* **65**, 952–962 (1998)
23. Marghitu, D.B., Hurmuzlu, Y.: Three-dimensional rigid-body collisions with multiple contact points. *J. Appl. Mech.* **62**, 725–732 (1995)
24. Smith, C.E., Liu, P.-P.: Coefficient of restitution. *J. Appl. Mech.* **59**, 963–969 (1992)
25. Stoianovici, D., Hurmuzlu, Y.: A critical study of the applicability of rigid-body collision theory. *J. Appl. Mech.* **63**, 307–316 (1996)
26. Flores, P., Ambrosio, J., Claro, J.P.C., Lankaraki, H.M.: Translational joints with clearance in rigid multi-body systems. *J. Comput. Nonlinear Dyn.* **3**, 011007 (2008)
27. Erickson, D., Weber, M., Sharf, I.: Contact stiffness and damping estimation for robotic systems. *Int. J. Robot. Res.* **22**(1), 41–57 (2003)
28. Djerassi, S.: Collision with friction; part A: Newton's hypothesis. *Multibody Syst. Dyn.* **21**, 37–54 (2009). doi:[10.1007/s11044-008-9126-2](https://doi.org/10.1007/s11044-008-9126-2)
29. Boyce, E.W., DiPrima, C.R.: *Elementary Differential Equations*, 3rd edn. Wiley, New York (1977)
30. Neimark, J.I., Faev, N.A.: *Dynamics of Nonholonomic Systems*. American Math Society, Providence (1972)
31. Ferziger, T.H.: *Numerical Methods for Engineering Application*. Wiley, New York (1981)
32. Strang, G.: *Linear Algebra and Its Application*. Academic Press, New York (1980)